

## Supplementary Information

### Rapid-Response Flexible Gas Sensor Based on Porous MXene/In<sub>2</sub>O<sub>3</sub>

#### Composites with Integrated Heating for NO<sub>2</sub> Detection

Baichuan Sun<sup>a</sup>, Gaobin Xu<sup>a\*</sup>, Hongda Liu<sup>a</sup>, Cunhe Guan<sup>a</sup>, Shirong Chen<sup>a</sup>, Xing Chen<sup>a</sup>, Yuanming Ma<sup>a</sup>, Feixiang Tang<sup>a</sup>, Zhaohui Yang<sup>b</sup>

<sup>a</sup>*Micro Electromechanical System Research Center of Engineering and Technology of Anhui Province, School of Microelectronics, Hefei University of Technology, Hefei, Anhui 230009, China.*

<sup>b</sup>*Anhui Polytechnic University, Wuhu 241000, China*

\*Corresponding author: Email: gbxu@hfut.edu.cn, Tel: +86-0551-62902263

Fig. S1 shows the XPS spectra of the PM/In<sub>2</sub>O<sub>3</sub> composite. Fig. S1(a)–(e) show the high-resolution spectra of F1s, O1s, C1s, In3d<sub>5/2</sub>, and Ti2p, respectively, and Fig. S1(f) shows the overall survey spectrum of the composite. These results confirm the coexistence of MXene and In<sub>2</sub>O<sub>3</sub> within the composite.

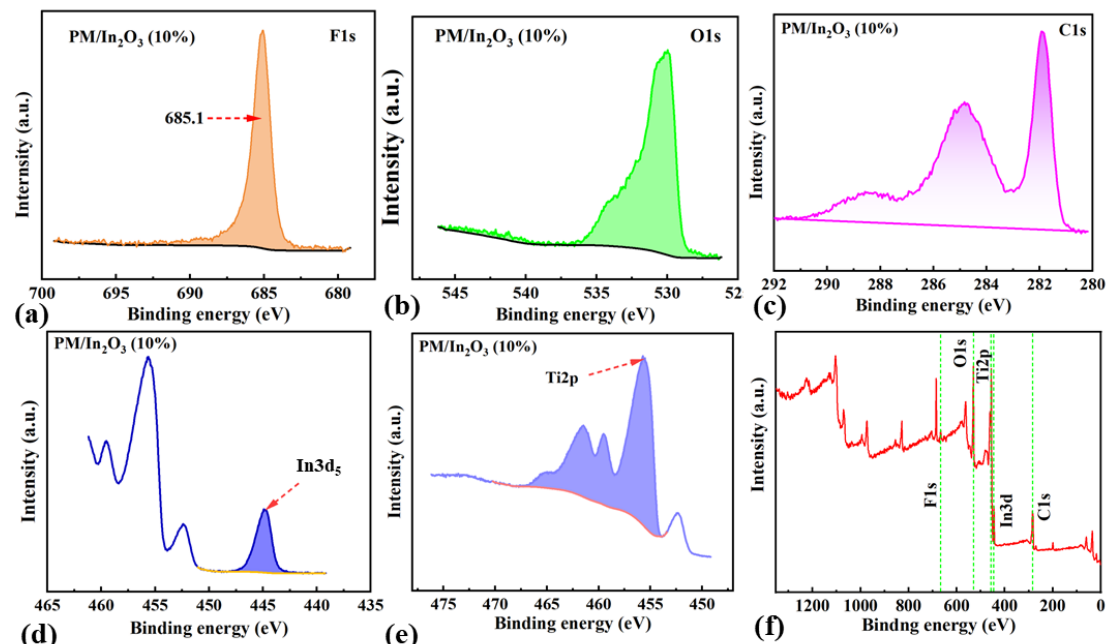


Fig. S1 XPS spectra of the PM/In<sub>2</sub>O<sub>3</sub> composite. (a–e) High-resolution spectra of F 1s, O 1s, C 1s, In 3d<sub>5/2</sub>, and Ti 2p, respectively; (f) overall survey spectrum of the composite.

Fig. S2 shows the pore size distributions of MXene, PM, and PM/In<sub>2</sub>O<sub>3</sub>.

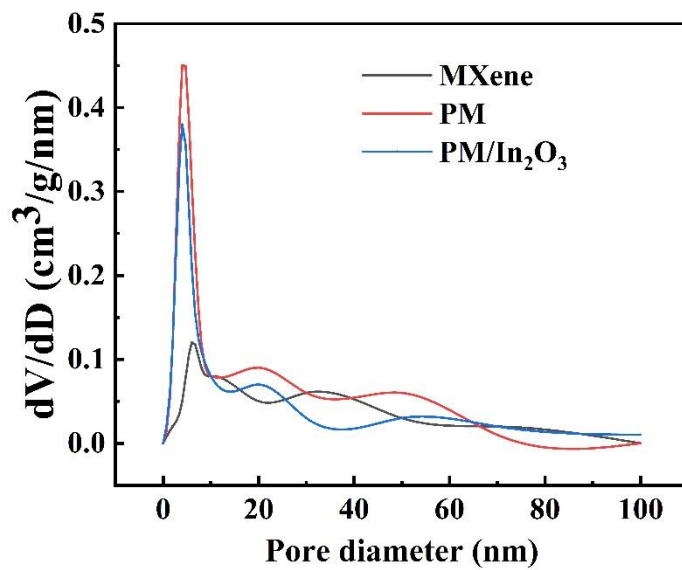


Fig. S2 Pore size distributions of MXene, PM, and PM/In<sub>2</sub>O<sub>3</sub>.

Fig. S3 illustrates the gas sensing performance of the device under a bending angle of 30° in comparison with the flat type. As shown in Fig. S3(a), the sensor maintains stable responses across various gas concentrations, consistently achieving reliable detection within the range of 0.01–100 ppm. Moreover, Fig. S3(b) reveals that the sensing results obtained under bent and flat states follow a strong linear relationship, expressed as  $y = 0.00367x + 1.0036$  with a correlation coefficient ( $R^2$ ) of 0.99. Such excellent agreement demonstrates that the FGS developed in this work can function reliably under moderate bending conditions, thereby ensuring applicability in scenarios involving curved surfaces.

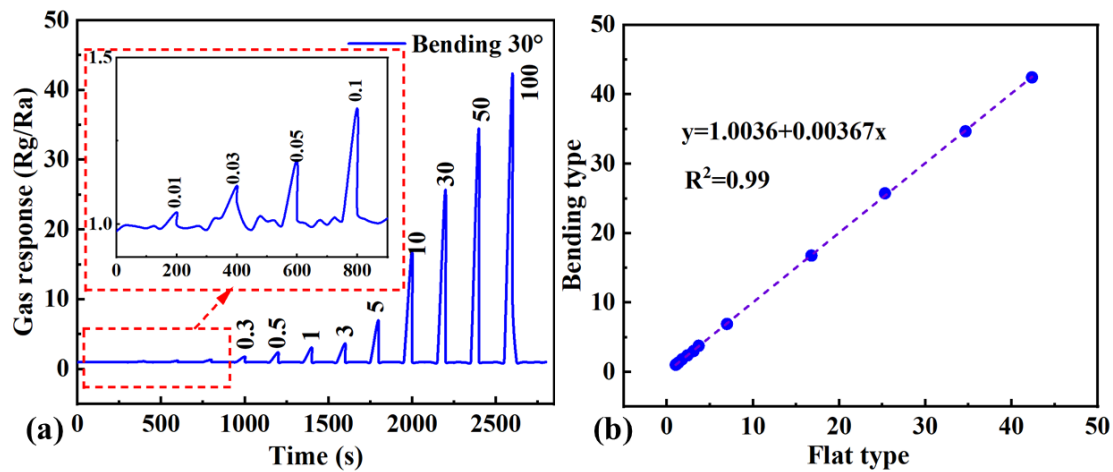


Figure S3. Gas sensing performance of the FGS under 30° bending compared with the flat type: (a) responses at different concentrations; (b) correlation between bent and flat types.

Table S1 The contents of the different oxygen species in PM, PM/In<sub>2</sub>O<sub>3</sub> and PM/In<sub>2</sub>O<sub>3</sub>-

$\text{NO}_2$ .

Oxygen species	PM (%)	PM/ $\text{In}_2\text{O}_3$ (%)	PM/ $\text{In}_2\text{O}_3\text{-NO}_2$ (%)
$\text{O}_1$	36.98	42.12	41.71
$\text{O}_d$	23.46	28.25	34.28
$\text{O}_a$	39.56	29.63	24.01